

# LOSSLESS REGION-BASED MULTISPECTRAL IMAGE COMPRESSION

G. Fernández i Ubierno

Swiss Federal Institute of Technology, Switzerland

## 1 INTRODUCTION

In this paper we present a lossless coding scheme for multispectral images. The algorithm differs from classical lossless approaches of multispectral image coding (1, 2, 3) in the fact that it is based on an independent coding of spectrally homogeneous regions. Regions that present a common multispectral signature are segmented. Then, spectral prediction is performed within these regions and finally spatial prediction removes the remaining correlation in the error images. This spatial prediction is also performed inside the regions by a region growing prediction algorithm that exploits the spatial correlation within region boundaries.

The motivations of using a region-based approach are twofold: *i*) to achieve better coding performances by adaptively exploiting spectral redundancies and *ii*) to introduce region scalability functionality to multispectral coding, where regions of interest are coded differently according to user preferences.

In recent papers (4, 5), we already suggested the use of arbitrarily shaped regions of support in order to compress multispectral images. In a lossy framework, we proposed a region-based KLT resulting in better performances than classical block-based KLT approaches. Lossy algorithms are not applicable in many scientific fields due to precision constraints. For this reason we present a lossless method for the compression of multispectral images with arbitrarily shaped segments.

Typically, lossless multispectral image coding methods are based on linear prediction between spectral bands in order to remove the spectral redundancy. Pixels from a given band are used to predict the pixel values for another band. The prediction coefficients are usually calculated from the statistics of both images by least-square criteria. Such a prediction is optimal in the least-square sense for the whole image but, due to the different spectral signatures present in the scene, a considerable error may be produced in some regions. By introducing the notion of region-based spectral prediction, regions with similar spectral signature are taken as support for prediction. Optimality for each region is obtained and the prediction error is substantially reduced.

This paper is organized as follows. Section 2 discusses the possible multispectral segmentations. Section 3 proposes an ordering of the spectral bands

before spectral prediction. Spectral prediction is explained in Section 4 and a clustering method that optimizes this prediction is presented in Section 5. Finally, the spatial decorrelation step is discussed in Section 6 and simulation results are given in Section 7.

## 2 MULTISPECTRAL SEGMENTATION

Spectrally homogeneous regions can be obtained by multidimensional clustering in the spectral dimensions. Since one of the goals of the method is to introduce region functionalities according to the user needs, the segmentation part should be left up to the specific application. In this paper we report results for meteorological (6) and biological (7) applications. Obviously, the determination of the regions has a direct influence on the overall performance of the algorithm. For this reason, Section 5 discusses the use of a clustering algorithm that aims at optimizing the coding performances at the expense of a loss in region functionality.

## 3 BAND ORDERING

An ordering of the spectral bands is proposed before the actual spectral prediction. The fact is that the *natural* order <sup>1</sup> of the spectral bands does not necessarily produce the best prediction performances. For instance, in remote sensing applications, bands located in the vapor absorption window (600-700nm) present very poor correlation with respect to the rest of the bands. However, bands located in the neighboring wavelengths, even if not being consecutive bands, present higher correlation. Moreover, it may happen that a given band is the best predictor for several bands. The simple natural ordering would never allow multiple prediction of several bands from a single band.

To cope with these problems an ordering based on a weighted directed graph was proposed by Tate (2). Graph weights were equal to the costs related to code the images with or without a given band. The drawback of this method was the need of computing all the coding costs possibilities beforehand.

We propose a band ordering based on the mutual information between bands. Mutual information (8)

---

<sup>1</sup>Natural order refers to the order given by the spectral wavelengths.

of two random variables  $X$  and  $Y$  ( $I(X; Y)$ ) can be interpreted as a measure of reduction of uncertainty of a variable  $X$  due to the knowledge of  $Y$ . It can be expressed as:

$$I(X; Y) = H(X) - H(X/Y) = H(Y) - H(Y/X), \quad (1)$$

where  $H()$  and  $H(/)$  are respectively the entropy and conditional entropy.  $I(X; Y)$  is symmetrical, since  $X$  reduces the uncertainty of  $Y$  as much as  $Y$  reduces it for  $X$ . In other words,  $I(X; Y)$  expresses the maximum number of bits per sample that can be saved by predicting  $X$  from  $Y$  and vice-versa.

For obtaining such a band ordering the matrix of the mutual information between all the bands must be computed. Mutual information values are graph weights of a weighted graph where each spectral band is in a vertex. Figure 1.a shows a 5-band example. Since  $I(X; Y)$  is symmetrical, the graph does not need to be directed and the optimal sequence can be obtained by the maximum-weight spanning tree (9). In other words, the sequence that saves the maximum amount of bits per sample during the prediction process is obtained. The algorithm ends up giving a sequence of relationships between spectral bands. Once the maximum weighted tree is obtained, prediction starts from the band in the most weighted edge that has lower entropy. Figure 1.b shows the final directed tree.

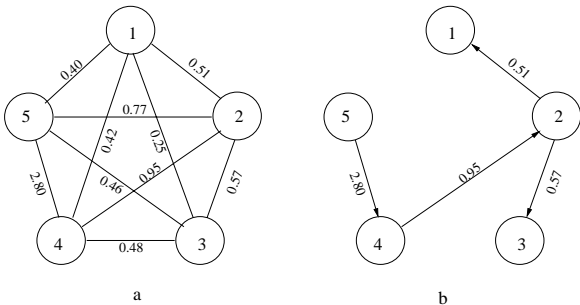


Figure 1: *a.* Mutual information weighted graph, *b.* Maximum-weight (directed) spanning tree.

In order to be consistent with the region-based approach, band ordering is based on region statistics rather than *whole image* statistics. Thus, the same algorithm is applied using regions instead of complete bands. In this way, different regions in a given band can be predicted from different bands depending on region statistics.

The computation of the mutual information matrix may imply an expensive and complex procedure, especially for a large number of bands. Fortunately, the relationships between spectral bands for a given multispectral system do not change significantly. In this case, a non-adaptive band ordering can be pre-computed and optimized from a training dataset.

Another possibility is to use the correlation factor instead of mutual information. It is simpler to compute, but its meaning is not directly connected to uncertainty reduction.

#### 4 SPECTRAL PREDICTION

Spectral prediction can be done by approximating the predicted band by a polynomial function of the reference one. For a  $(x, y)$  pixel position:

$$\hat{b}_a(x, y) = \sum_{i=0}^M a_i * b_b(x, y)^i, \quad (2)$$

where band  $b_a$  is predicted from band  $b_b$  by means of an  $M$ th order polynomial. In our case, the prediction order ( $M$ ) is fixed to one, since inter-band correlation is generally linear. Experimental results showed that the improvements brought by adding a 2nd order term to the prediction were not worth the complexity and overhead cost (10). Thus, spectral prediction is restricted to the following equation:

$$\hat{b}_a(x, y) = \alpha * b_b(x, y) + \beta, \quad (3)$$

where  $\alpha$  and  $\beta$  are the prediction coefficients obtained with a least-squares criterion (11), expressed by:

$$Q = E[(b_a - \hat{b}_a)^2] = E[(b_a - (\alpha * b_b + \beta))^2]. \quad (4)$$

By canceling the partial derivatives of  $Q$  with respect to  $\alpha$  and  $\beta$ , the prediction values are extracted. This procedure is exactly the same as the one of fitting a set of data points to a straight-line model (known as *linear regression*). Pixels belonging to the same region are fitted with the same linear model and a different model is computed for each region. The spectral homogeneity of the regions is a determining factor for producing a successful prediction.

#### 5 CLUSTERING FOR SPECTRAL DECORRELATION OPTIMIZATION

In Section 2 it was mentioned that the multispectral segmentation should be related to the application needs. However, it is reasonable to expect that each multispectral segmentation will perform differently depending on the spectral homogeneity of the regions. In this section we present a clustering scheme that aims at optimizing the performances of the coding method. Obviously, the regions defined in this way will lose the functionality feature with respect to the application.

Ideally, in order to exploit the linear prediction model, multispectral clusters should have a linear relationship within all the bands. With that constraint in mind, one can define a clustering algorithm that

determines linear (ellipsoidal) shaped clusters in the  $N$ -dimensional spectral space.

Such a clustering scheme works in the following way. Given an arbitrary initial segmentation, a different Karhunen-Loève Transform (KLT) is computed in the spectral dimension from the pixels of each class. The method iteratively checks all pixels and it moves them from one class to another if the coefficients in the KLT of the new class minimize the following objective function:

$$J_i = \sum_{j=2}^N c_{ij}^2, \quad (5)$$

where  $N$  is the dimension of the space (number of bands) and  $c_{ij}$  the  $j$ th coefficient for the given pixel computed for the  $i$ th KLT. In other words, the clustering minimizes the variance over all the transformed components except the main one, leading to ellipsoidal clusters centered around their main component vector. KLTs are recomputed after all pixels have been checked and the process starts again until the obtained main vectors do not change at a certain precision. The resulting segmentation provides classes whose spectral relationship is approximately linear.

## 6 REGION GROWING SPATIAL PREDICTION

Error images obtained after spectral prediction still have spatial correlation to be exploited. Classical 2D prediction as the one used in the lossless JPEG standard (12) do not allow an efficient region-based spatial coding because they are based on a fixed neighborhood for predicting a pixel.

The classical spatial prediction can be summarized as follows: in order to predict a pixel value, consider its neighbors in a causal manner (left and top side depending on the scan sequence), combine them in order to produce an estimate of the present pixel value, round this prediction to the nearest integer and subtract it from the actual value. The obtained error is called prediction error. Prediction algorithms differ in the way the neighbors are combined. For instance, JPEG may combine the neighbors in 7 different ways. Performances of each predictor depend upon image structure.

In the present compression scheme, spatial prediction should be performed from pixel neighbors belonging to the same region in order to avoid an erroneous estimation at region boundaries. The problem is that, due to the arbitrary shape of the regions, classical scanning sequences (as top-right/bottom-left) do not assure a correct prediction for all pixels in the region. For the mentioned reasons, a 2D decorrelation based on a region growing algorithm is proposed. Pixels inside the region are "scanned" in the same way as

in region growing but only the neighbor pixels that have already been scanned are used for the spatial prediction. The process is illustrated in Figure 2, and can be summarized in the following steps:

- (i) define the spatial regions  $r_1, r_2, \dots, r_n$ ;
- (ii) locate the first point belonging to  $r_1$ , put its value on the final bit-stream (no prediction possible for the first point);
- (iii) put its 4-connected neighbors that belong to  $r_1$  on a queue and label them as "stacked". Label the current pixel as "scanned" (dark region);
- (iv) extract the next pixel from the queue in a FIFO manner, look at the 4-connected neighbors and make a prediction from the ones that are labeled as "scanned". Round the prediction to the nearest integer and compute the prediction error;
- (v) back to (iii) until all pixels of  $r_1$  are scanned;
- (vi) repeat the procedure for the other regions.

In the illustrated example of Figure 2, pixel 12 is about to be predicted, its 4-connected neighbors are stored in the stack (pixels 19 and 18, 17 was already stacked by pixel 11 and 7 is labeled as "scanned"). The prediction is produced from the scanned neighbor (pixel 7).

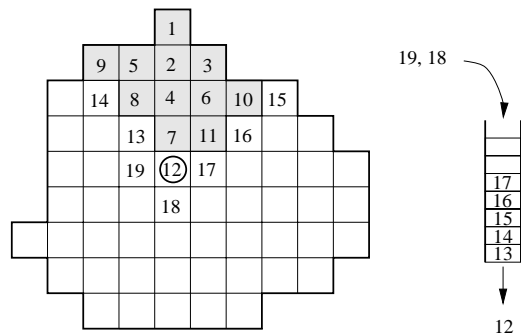


Figure 2: Region growing spatial prediction, see text for details.

With the presented method, spatial prediction is always performed from neighboring pixels belonging to the same region. The number of neighbors used for prediction is thus variable depending on the pixel position inside a region. Neighbor connectivity can be extended to 8 and the same method applies.

## 7 RESULTS

### 7.1 Spectral and spatial decorrelation

We report results for two multispectral datasets, the 5-band GOES imager instrument and the 7-band Thematic Mapper.

We compare different spectral decorrelators: prediction without regions, prediction using a block-based

partition of  $64 * 64$  pixels and region-based prediction using the clustering algorithm of Section 5 with 3 classes. Performance measures are given in terms of entropy of prediction error images. Table 1 list the results after spectral prediction. The gain of ordering the bands is about 7% whereas the gains of the region-based prediction with respect to non-region or block-based prediction are 10.1% and 8.8% respectively.

Table 1: Entropy of residual error after spectral prediction.

|                      | 5-band GOES | 7-band TM |
|----------------------|-------------|-----------|
| original             | 6.44        | 5.41      |
| no regions, no order | 6.78        | 4.75      |
| no regions           | 6.13        | 4.60      |
| block                | 6.01        | 4.56      |
| 3 regions            | 5.46        | 4.17      |

The following results are related to the region growing spatial prediction. Table 2 shows the entropy of the error after spatial prediction. Averaged gains of the region-based approach are of 4.85% and 4.65% in entropy with respect to non-region and block-based approaches.

Table 2: Entropy of residual error after spatial prediction.

|            | 5-band GOES | 7-band TM |
|------------|-------------|-----------|
| no regions | 4.16        | 3.56      |
| block      | 4.11        | 3.59      |
| 3 regions  | 3.86        | 3.47      |

In summary, a region-based spectral and spatial decorrelation after band ordering is the approach that yields prediction errors with the lowest variance and entropy. Globally, variance has been reduced by more than 95% and entropy by 37%. This reduction is due to the three different processing step: band ordering, region-based spectral prediction and region-based spatial prediction. Simulation results show that spectral and spatial decorrelation each account for 40-50% of the total reduction, and that band ordering is responsible for 10-20% of the overall reduction.

## 7.2 Compression results

Compression performances of each spectral decorrelation method are given in this section. Prediction error is entropy-coded and it is compared with the standard JPEG in its lossless form.

JPEG has 7 different prediction modes, each one giving different performances depending upon image structure. Each multispectral band was independently coded by the predictor that gave the best

performance for the particular band. The average compression ratio for all the bands was computed for comparison with respect to the other algorithms.

In Table 3 compression ratios for each one of the coders are presented. Results include overhead due to spectral prediction parameters and segmentation cost when needed. In the table, the influence of each processing step on the final bit-rate can be observed. The simplest *non-region/non band ordering* approach already improves JPEG by a 5 – 11% (effect of spectral prediction). By introducing the features of band ordering and region-based prediction the coder outperforms JPEG by 15%. The relative performances between the non-region, block-based and region-based spectral prediction, can also be compared.

Table 3: Compression ratio for several coding approaches and two different datasets.

|                      | 5-band GOES | 7-band TM |
|----------------------|-------------|-----------|
| jpeg                 | 1.96        | 2.0       |
| no regions, no order | 2.07        | 2.23      |
| no regions           | 2.14        | 2.27      |
| block                | 2.15        | 2.25      |
| 3 regions            | 2.26        | 2.32      |

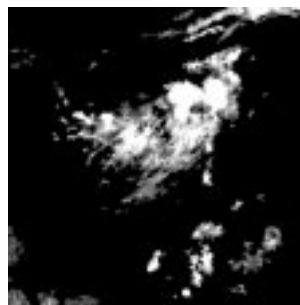


Figure 3: Regions of interest coded independently from the background for the cloud (*left*) and cells (*right*) application.

Finally, evaluation results for the region scalability feature are given. Two multispectral applications define different regions of interest (ROIs). The first application is related to cloud analysis (6) with 5 bands whereas the second one is related to cellular image analysis (7) with 3 bands. The regions of interest (clouds and cells respectively) were extracted from the background. The multispectral images were coded with the different approaches. Tables 4 and 5 show the composition in bytes of the bit-stream for each method, as well as the compression ratio and the average bit/pixel/band.

For the cloud example, the region-based approach saves 137.3KB with respect to the standard lossless JPEG (improvement of 41.1%) whereas for the cell

Table 4: Results of a lossless coding of the cloud ROI.

|          | JPEG   | no region | block  | region |
|----------|--------|-----------|--------|--------|
| mask     | -      | -         | -      | 1962   |
| overhead | -      | 98        | 2204   | 98     |
| data     | 342470 | 235806    | 264028 | 199751 |
| total    | 342470 | 235904    | 266232 | 201811 |
| cr.      | 3.82   | 5.55      | 4.92   | 6.495  |
| b/p/b    | 2.090  | 1.439     | 1.624  | 1.231  |

Table 5: Results of a lossless coding of the cell ROI.

|          | JPEG   | no region | block | region |
|----------|--------|-----------|-------|--------|
| mask     | -      | -         | -     | 2128   |
| overhead | -      | 84        | 1558  | 82     |
| data     | 146008 | 73698     | 75013 | 37556  |
| total    | 146008 | 73782     | 76571 | 39766  |
| cr.      | 5.51   | 10.91     | 10.5  | 20.24  |
| b/p/b    | 1.45   | 0.733     | 0.76  | 0.39   |

example the saving is of 103.75KB (improvement of 72.7%).

## 8 CONCLUSIONS

In this paper we have presented a new approach for the lossless compression of multispectral images based on arbitrarily shaped segments. The algorithm is able to adaptively exploit the existing spectral correlation between bands. A band ordering based on mutual information is applied prior to linear spectral prediction based on statistics of the regions. Finally, regions are spatially decorrelated by an adaptive 2D prediction. In addition to that, a clustering algorithm that aims at optimizing the performances of the coder has also been presented.

Results show that spectral prediction performed within homogeneous regions is more efficient than performed on the whole image or even on a block-based partition. Finally, after the shape adaptive spatial prediction stage, compression ratios are slightly better than those of classical lossless multispectral approaches. Standard lossless JPEG algorithm is improved by 15%. To this improvement in performance one may add the new functionality that the presented algorithm introduces, where only the regions of interest can be coded according to user preferences.

## REFERENCES

1. N. D. Memon, K. Sayood, and S. S. Magliveiras. "Lossless compression of multispectral image data". *IEEE Transactions on Geoscience and Remote Sensing*, Vol. 32, No. 2, pp. 282–289, March 1994.
2. S.R. Tate. "Band ordering in lossless compression of multispectral images". In *Proceedings of Data Compression Conference*, pp. 311–320, Snowbird, Utah, March 1994.
3. R.E. Roger and M.C. Cavenor. "Lossless compression of AVIRIS images". *IEEE Transactions on Image Processing*, Vol. 5, No. 5, pp. 713–19, May 1996.
4. G. Fernández and C. M. Wittenbrink. "Region based KLT for multispectral image compression". In *8th European Signal Processing Conference EUSIPCO 96*, Vol. 1, pp. 355–358, Trieste, Italy, September 1996.
5. G. Fernández and C. M. Wittenbrink. "Coding spectrally homogeneous regions in multispectral image compression". In *Proceedings of International Conference on Image Processing, ICIP'96*, Vol. 2, pp. 923–6, Lausanne, Switzerland, September 1996.
6. C. M. Wittenbrink, G. Fernández, and G. G. Langdon. "Feature extraction of clouds from GOES satellite data for integrated model measurement visualization". In *Proceedings of SPIE/IS&T Conference: Image and Video Processing IV*, Vol. 2666, pp. 212–222, San Jose, February 1996.
7. G. Fernández, M. Kunt, and J-P. Zryd. "Multi-spectral based cell segmentation and analysis". In *Proc. of the Workshop on Physics-Based Modeling in Computer Vision*, pp. 166–172, Cambridge, MA, June 1995.
8. T.M. Cover and J.A. Thomas. *Elements of information theory*. John Wiley & Sons, 1991.
9. R. J. Wilson. *Introduction to graph theory*. Longman Group Ltd., 3rd edition, 1985.
10. J. Lee. "Least squares approach for predictive coding of 3-d images". In *Proceedings of International Conference on Image Processing, ICIP'96*, pp. 311–320, Lausanne, Switzerland, September 1996.
11. A. Papoulis. *Probability and statistics*. Prentice-Hall International, Inc., 1990.
12. G. K. Wallace. "The JPEG still image compression standard". *Communications of the ACM*, Vol. 34, No. 4, pp. 30–44, April 1991.